

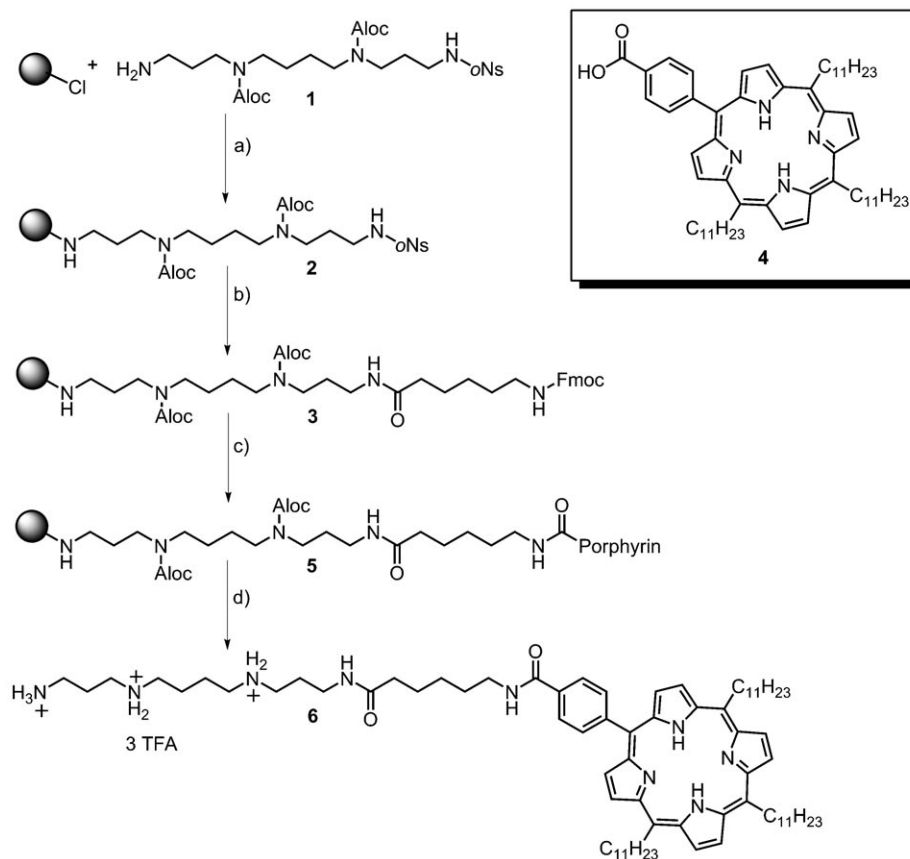
DOI: 10.1002/cmdc.200800013

## Conjugation of Spermine Facilitates Cellular Uptake and Enhances Antitumor and Antibiotic Properties of Highly Lipophilic Porphyrins

Frank Hahn,<sup>[a]</sup> Katja Schmitz,<sup>[b, c]</sup> Teodor S. Balaban,<sup>[c]</sup> Stefan Bräse,<sup>\*,[b]</sup> and Ute Schepers<sup>\*,[a]</sup>

Recently, a great deal of attention has been focused on photodynamic therapy (PDT), in which the administration of photosensitizers, and subsequent irradiation of the target area, leads to the initiation of a radical reaction and ultimately cell death.<sup>[1]</sup> PDT can be used to treat a variety of conditions such as age-related macular degeneration, various skin disorders, and an increasing number of cancers.<sup>[2]</sup> Other applications for PDT are also under investigation, although in various stages of development, for example, as a nonclassical antibiotic against pathogenic micro-organisms such as bacteria and yeast strains, or as an antiviral treatment.<sup>[3]</sup> Most of the porphyrin compounds with good uptake rates contain either lipophilic or polycationic side chains. More lipophilic porphyrins often enhance the PDT effect; their ability to interact with the hydrophobic chains of lipids in the cell membrane leads to a significant disorder in the bilayer structure. In contrast, polycationic side chains enhance the water solubility of the porphyrin and can promote a tight electrostatic interaction with negatively charged sites, mainly proteoglycans, on the

outer surface of cell membranes for nonspecific endocytosis.<sup>[4]</sup> Generally, the inclusion of cationic moieties leads to an accu-



**Scheme 1.** Solid-phase synthesis of polyamine-coupled porphyrin **6**: a) *bis*-Aloc-nosyl-spermine (**1**) (10 equiv), DIPEA, CH<sub>2</sub>Cl<sub>2</sub>, 8 h, RT; b) 2-thioethanol (20 equiv), DBU (20 equiv), DMF, 20 h, RT; c) *N*-Fmoc-amino-hexanoic acid (3 equiv), PyBrOP (2 equiv), DIPEA (4 equiv) in DMF, 20 h, RT; c) 1) piperidine in DMF (20%), 3 × 2 min, RT; c) 2) carboxy-porphyrin **4** (2 equiv), HOBT (3.4 equiv), DCC (5 equiv), CH<sub>2</sub>Cl<sub>2</sub>/DMF (1:1, (v/v)) 5 d, RT; d) 1) *N,N'*-dimethylbarbituric acid (10 equiv), Pd(PPh<sub>3</sub>)<sub>4</sub> (20 mol%), CH<sub>2</sub>Cl<sub>2</sub>, 3 h, 40 °C; 2) TFA in CH<sub>2</sub>Cl<sub>2</sub> (10%), RT.

[a] F. Hahn, Dr. U. Schepers  
Kekulé-Institut für Organische Chemie und Biochemie, LIMES Institute  
Program Unit Membrane Biology and Lipid Biochemistry  
Rheinische Friedrich Wilhelms Universität Bonn  
Gerhard Domagk Str. 1, 53121 Bonn (Germany)  
Fax: (+49) 228-73-7778  
E-mail: schepers@uni-bonn.de

[b] Dr. K. Schmitz, Prof. Dr. S. Bräse  
Institut für Organische Chemie, Universität Karlsruhe (TH)  
Fritz-Haber-Weg 6, 76131 Karlsruhe (Germany)  
Fax: (+49) 721-608-8581  
E-mail: braese@ioc.uka.de

[c] Dr. K. Schmitz, Prof. Dr. T. S. Balaban  
Forschungszentrum Karlsruhe, 76021 Karlsruhe (Germany)

Supporting information for this article is available on the WWW under <http://dx.doi.org/10.1002/cmdc.200800013>.

mulation of drug in the endosomal and lysosomal compartments, however targeting of the porphyrins to mitochondria might further enhance their phototoxic effect. Furthermore, binding and photodynamic efficiencies were found to be inversely proportional to the number of positively charged groups, and directly proportional to *n*-octanol/water partition coefficients;<sup>[5]</sup> amphiphilic porphyrins with low cationic charge are suggested to improve both features.

The physicochemical properties of amphiphilic porphyrins make them difficult to purify for *in vivo* application. Herein, we report the solid-phase synthesis of a spermine-porphyrin conjugate, containing three highly hydrophobic undecanyl side chains, as a model amphiphilic porphyrin (Scheme 1). The or-

thogonal protection of the primary and secondary amino groups allows the unidirectional elongation of the polyamine chain without by-product formation, and the final product is obtained from the solid support without the need for further purification. This synthetic route would permit the generation of a library of amphiphilic photoactive compounds. The orthogonally protected building block, *bis*-Aloc-nosyl-spermine **1**, was attached to the 2-chlorotrityl resin under basic conditions. Deprotection of the primary amine, and subsequent coupling to *N*-Fmoc-aminohexanoic acid extended the chain to give compound **3**. This C<sub>6</sub> spacer was intended to attenuate interactions of the spermine side chain with the porphyrin moiety, yielding more flexibility for the porphyrin to penetrate into the membrane. After Fmoc deprotection, carboxy-porphyrin **4** was coupled to the N-terminal end to give the resin-bound compound, **5**. Cleavage from the resin using trifluoroacetic acid gave the amphiphilic porphyrin **6**.

The polyamine side chain greatly enhanced the solubility of the lipophilic porphyrin. While **4** was insoluble in water and only poorly soluble in methanol (<40 μM), **6** exhibited excellent solubility (>20 mM) in water and methanol. To determine whether **6** aggregates nonspecifically, we studied solutions of different concentrations in methylene chloride and in deionized water. Upon dilution, no changes in the Soret or Q bands were observed, indicating that the amphiphilic conjugate **6** is fully solvated (Supporting Information, figures S4–8). Uptake experiments were performed in HeLa cells, human primary fibroblasts, and COS7 cells at 0.1, 0.5, 1, 5, 20, 50, and 100 μM. After 4, 16, 24, and 48 h the cells were analyzed by live imaging, to avoid artificial diffusion due to membrane perforation during fixation (Figure 1, and Supporting Information, figures

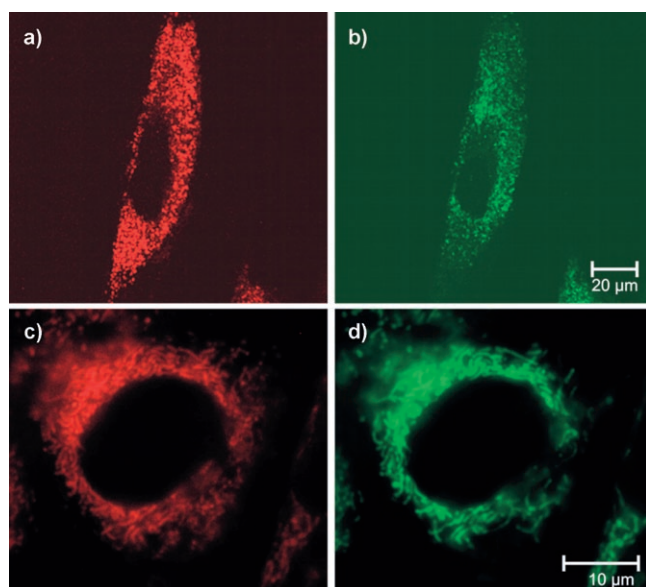


**Figure 1.** Fluorescence and confocal microscopy of cells after treatment with **6** (5 μM) and organelle staining: a) living human primary fibroblasts; b) living human primary fibroblasts co-stained with 150 nM LysoTracker green for 1 h to label the endosomal-lysosomal compartment; c) HeLa cells; d) HeLa cells co-stained with Mitotracker green for 1 h to label the mitochondria (Supporting Information, figures S1–3).

S1–3), or by fluorimetry, to measure the uptake (Figure 2). Almost all cells showed an accumulation of **6** on the surface or within the cells, and after treatment with high concentrations (50, 100 μM), daylight was sufficient to kill the majority of cells within 5–30 min.

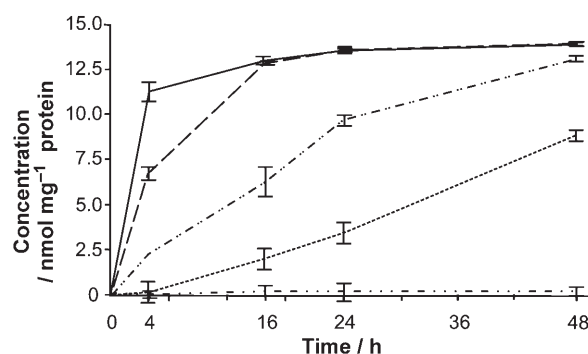


**Figure 2.** Time- and concentration-dependent uptake of polyamine-coupled porphyrin **6** and porphyrin **4** in HeLa cells (**6**, 10 μM, —; **6**, 5 μM, ---; **6**, 1 μM, - - -; **6**, 0.5 μM, - - - -; **4**, 5 μM, - - - - -). To determine the polyamine-porphyrin concentration, fluorescence emission was read at 420/650 nm (excitation/emission) by using a ThermoScientific Varioskan plate reader. The emissions of *n* = 4 experiments were quantified and normalized to the amount of the total protein, and the SD was calculated.

As opposed to **4**, which could not be detected inside the cells at a concentration of 5 μM, **6** exhibited a highly improved cellular uptake at the same concentration and increased with incubation time (Figures 1 and 2). Here, it should be mentioned that the final methanol concentration in the media is 10% after treatment with **4** (5 μM), which is unsuitable for cell culture and in vivo application. Equivalent treatment of the cells with **6** and 10% methanol concentration still showed efficient uptake but also decreased the cell viability to <50%. Cellular uptake of **6** could be observed by fluorescence microscopy and fluorimetric determination for concentrations as low as 0.5 μM in almost all cells with increasing levels over time, implying a slow uptake of the membrane-attached compound (Figures 1 and 2). As observed in confocal microscopy, the porphyrin fluorescence was restricted to structures that accumulate in the perinuclear region of the cell (Figure 1). Co-localization studies of **6** with endosomal/lysosomal markers revealed no co-localization with the endosomal compartment but rather with other vesicular-like compartments, different from lysosomes. Studies in HeLa cells using shorter incubation times and a lower concentration (1 μM) indicated co-localization with mitochondria (Figure 1). HeLa cells did not show the labeling of other vesicular structures as observed in the fibroblasts. Increasing concentration of **6** in HeLa cells shows an increase in mitochondria fragmentation close to the perinuclear region, probably due to the dark toxicity as measured in Figure 4c.

Recently, the rapid delivery of especially amphiphilic cations, including guanidyl-porphyrins,<sup>[6,7]</sup> to mitochondria has been reported. The cation rapidly accumulates in the mitochondria due to their highly negative membrane potential, while the hydrophobic moiety is believed to help with the integration into

the lipid bilayer.<sup>[6]</sup> Studies on the dose- and time-dependent cellular uptake were performed in HeLa cells (Figure 2). Although **6** is already rapidly taken up by the cells at low concentrations, the uptake reaches a saturation after 16–24 h, depending on the initial concentration. Cells treated with **4** (5  $\mu\text{M}$ ) showed no significant uptake or accumulation of the drug. Figure 2 shows the time and concentration dependence of the uptake by the cells. At higher concentrations, the fluorescence appeared to reach saturation, and no further increase was observed even after longer exposure times. It is not clear whether this saturation is due to concentration quenching, or real saturation of the compound; however, HPLC quantification studies with other non-porphyrin spermine conjugates have shown similar saturation effects (unpublished data) and will be studied further.

To determine the cellular toxicity of **6**, cells were incubated with various concentrations of **6** and **4** for 4 and 24 h and irradiated at 650 nm (Figure 3). In cells treated with **6** at 5  $\mu\text{M}$ , severe phototoxicity was observed, with 70% of cells dead or necrotic after 5 min, and 100% cell death seen at 15 min. At lower concentrations, the dosed cells had to be incubated for a longer period prior to irradiation to induce similar cytotoxicity. Cell death was dependent on intracellular saturation and irradiation time; non-irradiated cells were not affected. The effective dose ( $\text{ED}_{50}$ ) for irradiation seemed to be dependent on the total amount of the internalized or membrane-bound drug. The dark toxicity of **6**, measured 72 h after dosing, was low compared to the phototoxicity observed (Figure 4). However, reported dark toxicity values for porphyrin derivatives coupled to polycationic peptides, which accumulate in the endosomal compartment, were lower.<sup>[7]</sup> It is assumed that the mitochondrial-localization of **6** is responsible for the higher toxicity, as has been shown for other mitochondria localized porphyrin derivatives.<sup>[7]</sup> Increasing concentration of **6** in HeLa cells led to an increase in mitochondria fragmentation close to the peri-

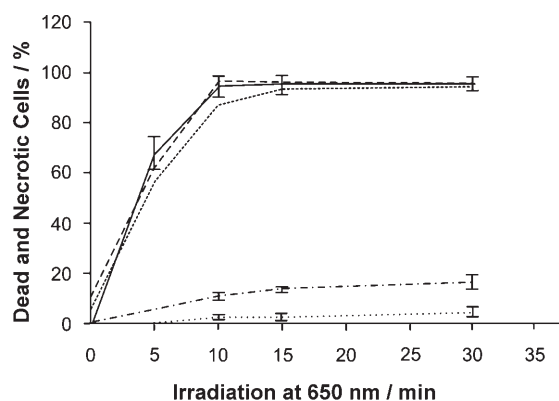


**Figure 3.** Quantification of the phototoxic effect of **6** and **4** on HeLa cells (**6**, 5  $\mu\text{M}$ , 4 h, —; **6**, 1  $\mu\text{M}$ , 24 h, ---; **6**, 0.1  $\mu\text{M}$ , 24 h, -----; **6**, 0.1  $\mu\text{M}$ , 4 h, -.-.-; **4**, 5  $\mu\text{M}$ , 4 h, .....). Quantification of dead and necrotic cells was performed after staining with propidium iodide and trypan blue. The irradiation of cells in the absence of photosensitizers did not trigger cell death. The cells were counted in  $3 \times 4$  random fields using the Axiovision software, and the read-out was evaluated by the Student's *t*-test. SD was calculated from  $n = 5$  experiments, except for data collected at 24 h which were obtained from a single experiment.

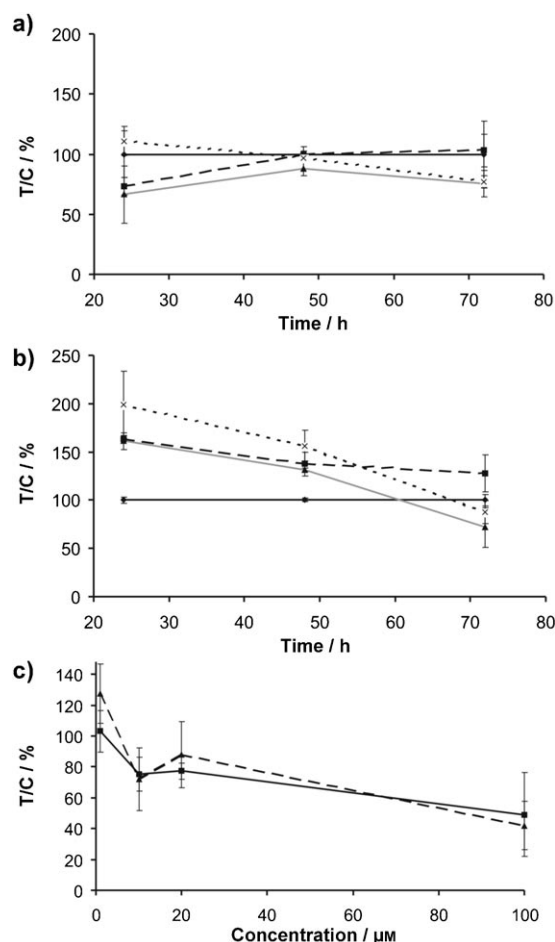


**Figure 4.** Dark toxicity of spermine–porphyrin **6** in a) primary human fibroblasts (0  $\mu\text{M}$  —; 1  $\mu\text{M}$  ---; 10  $\mu\text{M}$  —; 20  $\mu\text{M}$  -----); b) HeLa cells. The dark toxicity was measured at 24, 48, and 72 h after incubation with varying concentrations of **6**, and cell viability measured using the CellTiter96™ assay (0  $\mu\text{M}$  —; 1  $\mu\text{M}$  ---; 10  $\mu\text{M}$  —; 20  $\mu\text{M}$  -----); c) concentration-dependent dark toxicity after 72 h in HeLa cells (---) and primary human fibroblasts (—). T/C[%] = test over control (value for the viability of cells). SD was calculated from  $n = 3$  experiments.

nuclear region, probably due to the associated dark toxicity (Figure 4b,c). The same rationale might also explain the decreased dark toxicity in primary fibroblasts, where the drug is also localized in as yet undefined vesicular structures that do not co-localize with endosomes (Figure 4a). The dark toxicity  $\text{IC}_{50}$  values were measured after 72 h, as 81.2  $\mu\text{M}$  for HeLa cells, and 98.4  $\mu\text{M}$  for primary fibroblasts (Figure 4c).

Previously, a photodynamic approach was reported for the killing of bacteria at the skin surface, analogous to PDT for cancer.<sup>[8]</sup> A variety of compounds with photoactive properties have been tested against Gram-negative, and Gram-positive bacteria.<sup>[9]</sup> Anionic porphyrins showed no activity against either class of bacteria due to their poor cellular uptake and interaction with the bacterial cell wall. As it is well known that both Gram-positive bacteria and *E. coli* interact with positively charged peptides, we tested the phototoxic effect of cationic spermine–porphyrin **6** on *E. coli* and Gram-positive *Lactobacillus*. The amphiphilic porphyrin **6** showed efficient uptake by all

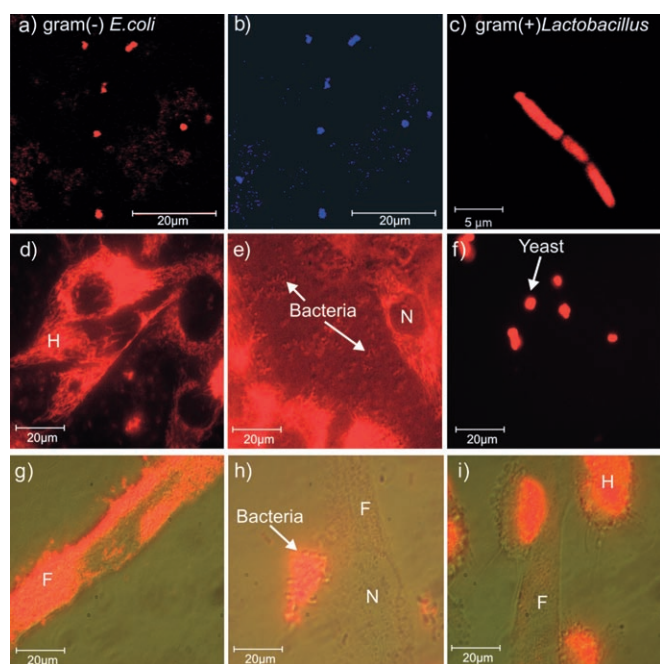


**Figure 5.** a) *E. coli* (Gram<sup>-</sup>), DAPI counterstain, **6** (1  $\mu\text{M}$ ) after 2 h; b) *E. coli*, DAPI counterstain, **6** (1  $\mu\text{M}$ ) after 2 h; c) *Lactobacillus* (Gram<sup>+</sup>), **6** (1  $\mu\text{M}$ ) after 2 h; d) non-infected HeLa cells; e) co-culture of tumor cells (HeLa) and Gram<sup>+</sup> bacteria; f) yeast cells **6** (1  $\mu\text{M}$ ) after 2 h; g) non-infected fibroblasts cells; h) co-culture of primary cells (human fibroblasts) and Gram<sup>+</sup> bacteria; i) HeLa cells, **6**, 1 h; H = HeLa cell, F = fibroblast; a–c, f, confocal images; d, e g–i, Nomarski images were merged with the fluorescent images of **6** (red).

cells tested, such as tumor and primary cells, Gram-positive and Gram-negative bacteria, and yeast (Figure 5). However, in a co-culture of bacteria and tumor cells, tumor cells preferentially bind and take up **6** (Figure 5e), while in a co-culture of bacteria and primary cells, the uptake of **6** by bacteria is prevalent even after 2 h. Likewise a co-culture of tumor cells and primary cells revealed a preferential uptake of **6** by tumor cells when treated with low concentrations and for short incubation times (Figure 5i). This observation is probably due to the increased density of negative charges on the outer membranes of primary cells over bacteria and tumor cells. So far, it is not clear whether the differences in uptake efficiencies are due to the interaction of the spermine moiety with the proteoglycans or negatively charged lipids on the cell surface, or whether the uptake depends on an active transport system such as the polyamine transporter. Nevertheless, this selectivity makes **6** a potential candidate for PDT, with less risk to healthy tissue. Further studies with multiresistant *Staphylococcus aureus* strains are ongoing.

In summary, solid-phase synthesis was used to synthesize an amphiphilic porphyrin with enhanced phototoxicity. Spermine was shown to solubilize lipophilic porphyrins and serve as a

molecular transporter, localizing the drug in mitochondria. This may be attributed to both the positively charged spermine moiety and the hydrophobic undecanyl chains of the porphyrin core. Following irradiation, this amphiphilic compound efficiently and selectively induced necrosis and apoptosis, in both tumor cells and bacteria over healthy cells, which makes amphiphilic porphyrin derivatives potential candidates for anti-cancer and antimicrobial photodynamic therapies.

## Acknowledgements

We thank the DFG -Center for Functional Nanostructures, Karlsruhe, and the Fond der Chemischen Industrie (K.S., Fellowship) for financial support, and Prof. Sandhoff, Bonn.

**Keywords:** amphiphilic porphyrins • antibiotics • molecular transporters • PDT • polyamines • solid-phase synthesis

- [1] a) C. M. Drain, B. Christensen, D. Mauzerall, *Proc. Natl. Acad. Sci. USA* **1989**, *86*, 6959–6962; b) R. K. Pandey in *Biomedical Photonics* (Ed.: V. D. Tuan), CRC, Boca Raton, **2002**.
- [2] a) I. J. MacDonald, T. J. Dougherty, *J. Porphyrins Phthalocyanines* **2001**, *5*, 105–129; b) R. Bonnett, *Chem. Soc. Rev.* **1995**, *24*, 19–33; c) Y. N. Konan, R. Gurny, E. Allemann, *J. Photochem. Photobiol. B* **2002**, *66*, 89–106; d) M. Momenteau, F. Lebras, B. Looock, *Tetrahedron Lett.* **1994**, *35*, 3289–3292; e) S. Hirohara, M. Obata, A. Saito, S. Ogata, C. Ohtsuki, S. Higashida, S. Ogura, I. Okura, Y. Sugai, Y. Mikata, M. Tanihara, S. Yano, *Photochem. Photobiol.* **2004**, *80*, 301–308.
- [3] a) J. P. Tome, M. G. Neves, A. C. Tome, J. A. Cavaleiro, M. Soncin, M. Magaraggia, S. Ferro, G. Jori, *J. Med. Chem.* **2004**, *47*, 6649–6652; b) J. M. Bliss, C. E. Bigelow, T. H. Foster, C. G. Haidaris, *Antimicrob. Agents Chemother.* **2004**, *48*, 2000–2006; c) A. R. Neurath, N. Strick, A. K. Debnath, *J. Mol. Recognit.* **1995**, *8*, 345–357; d) A. N. Vzorov, D. W. Dixon, J. S. Trommel, L. G. Marzilli, R. W. Compans, *Antimicrob. Agents Chemother.* **2002**, *46*, 3917–3925.
- [4] a) D. C. Mauzerall, C. M. Drain, *Biophys. J.* **1992**, *63*, 1544–1555; b) F. Ricchelli, L. Franchi, G. Miotto, L. Borsetto, S. Gobbo, P. Nikolov, J. C. Bommer, E. Reddi, *Int. J. Biochem. Cell Biol.* **2005**, *37*, 306–319.
- [5] a) M. Sibrian-Vazquez, T. J. Jensen, F. R. Fronczek, R. P. Hammer, M. G. H. Vicente, *Bioconjugate Chem.* **2005**, *16*, 852–863; b) F. M. Engelmann, S. V. O. Rocha, H. E. Toma, K. Araki, M. S. Baptista, *Int. J. Pharm.* **2007**, *329*, 12–18.
- [6] a) R. A. Smith, C. M. Porteous, A. M. Gane, M. P. Murphy, *Proc. Natl. Acad. Sci. USA* **2003**, *100*, 5407–5412; b) M. P. Murphy, R. A. Smith, *Annu. Rev. Pharmacol. Toxicol.* **2007**, *47*, 629–656.
- [7] a) T. Schröder, K. Schmitz, N. Niemeier, T. S. Balaban, H. F. Krug, U. Schepers, S. Bräse, *Bioconjugate Chem.* **2007**, *18*, 342–354; b) M. Sibrian-Vazquez, I. V. Nesterova, T. J. Jensen, M. G. Vicente, *Bioconjugate Chem.* **2008**, *19*, 705–713.
- [8] R. Fink-Puches, A. Hofer, J. Smolle, H. Kerl, P. Wolf, *J. Photochem. Photobiol. B* **1997**, *41*, 145–151.
- [9] a) M. Merchat, J. D. Spikes, G. Bertolini, G. Jori, *J. Photochem. Photobiol. B* **1996**, *35*, 149–157; b) M. Merchat, G. Bertolini, P. Giacomini, A. Villanueva, G. Jori, *J. Photochem. Photobiol. B* **1996**, *32*, 153–157.

Received: January 21, 2008

Revised: May 14, 2008

Published online on July 10, 2008